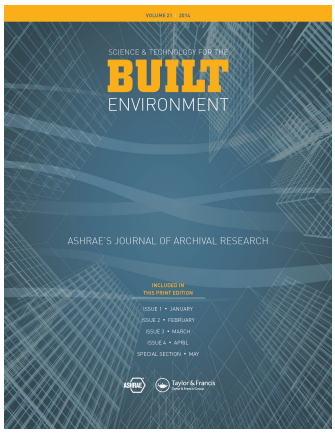

Science and Technology for the Built Environment
Publication details, including instructions for authors and subscription information:
http://www.tandfonline.com/loi/uhvc21

Modeling infection risk and energy use of upper-room Ultraviolet Germicidal Irradiation systems in multi-room environments

Catherine J. Noakes[a], M. Amirul I. Khan[a] & Carl A. Gilkeson[b]
[a] Pathogen Control Engineering Institute (PaCE), School of Civil Engineering, Faculty of Engineering, University of Leeds, Woodhouse Lane, LS2 9JT, LeedsUK
[b] Institute of Thermofluids, School of Mechanical Engineering, University of Leeds, Woodhouse Lane, LS2 9JT, LeedsUK
Published online: 06 Jan 2015.

Science and Technology for the Built Environment (2015) **21**, 99–111
Published with license by Taylor & Francis
ISSN: 2374-4731 print / 2374-474X online
DOI: 10.1080/10789669.2014.983035

Taylor & Francis
Taylor & Francis Group

Modeling infection risk and energy use of upper-room Ultraviolet Germicidal Irradiation systems in multi-room environments

CATHERINE J. NOAKES[1,*], M. AMIRUL I. KHAN[1], and CARL A. GILKESON[2]

[1]*Pathogen Control Engineering Institute (PaCE), School of Civil Engineering, Faculty of Engineering, University of Leeds, Woodhouse Lane, Leeds LS2 9JT, UK*
[2]*Institute of Thermofluids, School of Mechanical Engineering, University of Leeds, Woodhouse Lane, Leeds LS2 9JT, UK*

The effectiveness of ultraviolet irradiation at inactivating airborne pathogens is well proven, and the technology is also commonly promoted as an energy-efficient way of reducing infection risk in comparison to increasing ventilation. However, determining how and where to apply upper-room Ultraviolet Germicidal Irradiation devices for the greatest benefit is still poorly understood. This article links multi-zone infection risk models with energy calculations to assess the potential impact of a Ultraviolet Germicidal Irradiation installation across a series of inter-connected spaces, such as a hospital ward. A first-order decay model of ultraviolet inactivation is coupled with a room air model to simulate patient room and whole-ward level disinfection under different mixing and ultraviolet field conditions. Steady-state computation of quanta-concentrations is applied to the Wells–Riley equation to predict likely infection rates. Simulation of a hypothetical ward demonstrates the relative influence of different design factors for susceptible patients co-located with an infectious source or in nearby rooms. In each case, energy requirements are calculated and compared to achieving the same level of infection risk through improved ventilation. Ultraviolet devices are seen to be most effective where they are located close to the infectious source; however, when the location of the infectious source is not known, locating devices in patient rooms is likely to be more effective than installing them in connecting corridor or communal zones. Results show an ultraviolet system may be an energy-efficient solution to controlling airborne infection, particularly in semi-open hospital environments, and considering the whole ward rather than just a single room at the design stage is likely to lead to a more robust solution.

Introduction

It is well recognized that Ultraviolet Germicidal Irradiation (UVGI) systems can reduce the concentration of airborne pathogens in a room and, hence, reduce the risk of infection to occupants. Ultraviolet (UV-C) air disinfection is also commonly promoted as an energy-efficient way of reducing infection risk in comparison to increasing ventilation. However, determining how and where to apply UVGI devices for the greatest benefit is still poorly understood. Upper-room UVGI systems in particular have been advocated for their potential to minimize transmission in multi-occupant spaces. These systems deliver an open ultraviolet (UV) irradiation field to the upper zone of a room, created through baffled lamps located above the heads of occupants. Through ventilation flows and convective currents, airborne microorganisms in the room are circulated through this UV field and inactivated. Disinfection effectiveness has been demonstrated through laboratory studies in terms of reducing the level of viable microorganisms in the air (Miller et al. 2002) and directly in clinical studies where reduced rates of human to guinea pig transmission are reported (Escombe et al. 2009). While such data offer proof of performance, it is difficult to translate experimental findings into design of a system and the influence of different parameters.

Mathematical modeling offers a means of exploring design options and can consider impact on infection and device effectiveness. Several studies have sought to quantify the relationships between room airflow, UV power, and disinfection performance. Analytical models based on mixed airflow assumptions (Riley and Permutt 1971; Nicas and Miller 1999; Noakes et al. 2004a) have been applied to relate UV output and ventilation parameters to infection risk. These models assume uniform upper-zone UV irradiance and use coefficients to represent interzonal mixing. Despite their simplicity, they compare well to computational fluid dynamics (CFD)

Received April 28, 2014; accepted October 29, 2014
Catherine J. Noakes, PhD, CEng, is a Professor. **M. Amirul I. Khan, PhD**, is a Research Fellow. **Carl A. Gilkeson, PhD**, is a Teaching and Research Fellow.
*Corresponding author e-mail: C.J.Noakes@leeds.ac.uk

models (Noakes et al. 2004b) and are consistent with behavior measured in experimental studies (Miller et al. 2002). More recent studies have used CFD modeling to explore interaction between airflow, UV dose, and microorganism inactivation in greater detail (Noakes et al. 2004b, 2006; Sung and Kato 2010; Gilkeson and Noakes 2013; Zhu et al. 2013). These models enable a much more detailed assessment of the interaction between the local airflow pattern and a 3D upper-room UV field and can be used to assess the level of detail required in such a model (Gilkeson and Noakes 2013), risk to patients in hospital scenarios (Sung and Kato 2010), and effect of including a room mixing fan (Zhu et al. 2013).

Although these approaches enable quantification of the potential microbial reduction due to upper-room UV devices and their relationship with ventilation flows, they are all applied to single-room scenarios. The majority of indoor environments comprises multiple connected spaces and cannot be described through a single-zone model. Any spaces with transfer of air between them also have the potential for transfer of airborne infection. However, a control strategy implemented in one room will also have an impact on airborne infection risk in neighboring spaces, and this is likely a positive benefit. In the case of an upper-room UVGI system, could a wall- or ceiling-mounted upper-room device installed in just one room provide adequate protection to all occupants in a hospital ward, or is it necessary to install one or more of these devices in all rooms? Should upper-room UV devices also be installed in corridor/communal spaces, or just those rooms that are deemed to be high risk? Clearly installing more UV devices has a capital, energy, and maintenance cost, but is this justified? And how does a UVGI system compare to the conventional approach of increasing ventilation rates both in terms of potential for reducing infection risk and energy efficiency? Ultimately the decision to install a UV system may well be determined by financial constraints; however, those tasked with making the decision currently have limited means of making an assessment of the infection control benefits and the energy requirements of different numbers and locations of devices and how this compares to conventional ventilation approaches.

This article aims to develop a numerical model framework that can enable the combined evaluation of the likely airborne infection risk and energy requirements resulting from the installation of one or more upper-room UVGI devices within an inter-connected space, such as a hospital ward. A zonal mixing model is coupled with room-specific upper-zone average UV fields and a first-order microbial decay equation to simulate both UV dose and infectious microorganism distributions at room and ward levels. Infection risk to occupants is evaluated using the Wells–Riley model and is combined with annual energy calculations for a number of possible design scenarios to determine the influence of factors, including ventilation rate, number and location of UV devices, disease, and location of infectious source on both the infection risk and the energy use. This is used to show how the approach may aid the selection of a suitable design, at a whole-ward level, in terms of minimizing energy use and infection risk given a particular set of constraints.

Modeling approach

UV performance

UV-C irradiation damages the DNA of airborne microorganisms, resulting in mutations and, ultimately, cell death. The effectiveness of a UV system depends on both the dose of UV irradiation, or fluence, that an airborne microorganism receives and the species of microorganism. UV dose D (J/m^2) is a cumulative quantity that is defined as the product of the UV irradiance E (W/m^2) and the duration of exposure t (s):

$$D = Et. \tag{1}$$

This can be related to microorganism concentration over time through a decay model; in the simplest case, the fraction of airborne microorganisms remaining with time $\varphi(t)$ can be expressed as

$$\phi(t) = e^{-kD} = e^{-kEt}. \tag{2}$$

Here k is a microorganism susceptibility constant (m^2/J; sometimes denoted Z) that is species dependent and experimentally derived. Typical values for a range of microroganisms are presented in a number of sources, with Kowalski (2009) presenting the most comprehensive compilation of published values from numerous experimental studies. Equation 1 represents a first-order decay assumption that is realistic for many microorganisms, including *Mycobacterium tuberculosis* and other Mycobacterium species in air (Kowalski 2009). Other models incorporating a threshold dose or two-stage decay characteristics have been proposed for certain pathogens (Kowalski 2009).

Zonal mixing model

Modeling UV dose or microorganism inactivation in an upper-room UV system requires consideration of both the airflow and irradiance fields, as it is the interaction between the two that determines performance. The airflow model follows the zonal approaches described in Noakes et al. (2004a, 2004b) and Noakes and Sleigh (2009). Each room or bay within a hospital ward is treated as a two-zone space, with a lower occupied zone in room i (volume V_{Li}) comprising the larger part of the room and an upper zone (volume V_{Ui}) where UV fixtures are assumed to be located, as shown in Figure 1. Air within each zone is assumed to be fully mixed, but the transfer between upper and lower zones is assumed to be incomplete mixing and is characterized by a dimensionless mixing factor β (Beggs and Sleigh 2002). Ventilation air is assumed to be extracted from the lower zone at rate Q_i, and contaminant-free air supplied at the same rate to either the upper or lower zone. Flow between adjacent zones is characterized by an inter-room flow rate γ_{ij}. Both β and γ_{ij} are constant for a particular scenario, assuming that the within-room mixing and inter-room transfer is the same throughout the ward.

Infectious microorganisms in the air are modeled in terms of "infectious quanta," a commonly used term to represent

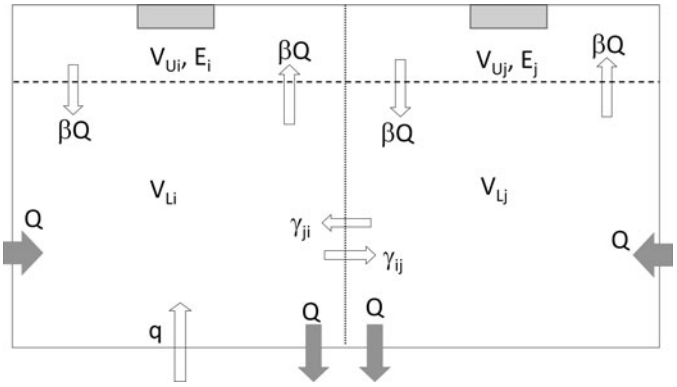

Fig. 1. Upper-room UV installation and model air mixing assumptions in two connected rooms, room *i* (left) and *j* (right). Case assumes air is supplied and extracted in the lower zone of each room and infectious sources are only present in room *i*.

concentration and infectiousness of a particular pathogen (Wells 1955). This is treated as a deterministic variable and is assumed to be released at a constant rate q_i (quanta/s) in the lower zone of any room containing I_i infectors. For the case shown schematically in Figure 1, the concentration of infectious quanta in the ith lower zone C_{Li} and upper zone C_{Ui} can be approximated by considering the quanta generation, ventilation removal, and inter-zonal transfers for each case to give Equations 3 and 4:

$$V_{Li}\frac{dC_{Li}}{dt} = q_i I_i - QC_{Li} - \beta QC_{Li} + \beta QC_{Ui} - \sum_j \gamma_{ij} C_{Li} + \sum_j \gamma_{ji} C_{Lj}, \quad (3)$$

$$V_{Ui}\frac{dC_{Ui}}{dt} = \beta QC_{Li} - \beta QC_{Ui} - kE_i V_{Ui} C_{Ui}. \quad (4)$$

Here the final term in Equation 4 expresses the rate of removal due to the upper-zone UV field. If an upper-room UV device is present in a room, an average irradiance E_i (W/m^2) is defined in the upper-zone of the room as detailed later. By differentiating Equation 2, this final rate term as a function of irradiance E_i and microorganism susceptibility constant k are obtained. The natural decay of microorganisms is not included in the model, as this is assumed to be the same with or without the presence of UV in the room.

As shown in Noakes et al. (2006), UV dose can also be treated as a non-diffusive cumulative scalar parameter to simulate the distribution of dose in a room. The same approach can be applied in a zonal ventilation model, in a similar way to modeling the concentration of infectious quanta. For the case shown in Figure 1, with ventilation air entering and leaving the lower zone of each room, the upper (D_{Ui}) and lower (D_{Li}) zone dose can be modeled for room i by Equations 5 and 6. The final term in Equation 6 represents the rate of increase of dose due to the upper-room irradiance field, which is the derivative of Equation 1, as shown in Noakes et al. (2006):

$$V_{Li}\frac{dD_{Li}}{dt} = -QD_{Li} - \beta QD_{Li} + \beta QD_{Ui} - \sum_j \gamma_{ij} D_{Li} + \sum_j \gamma_{ji} D_{Lj}, \quad (5)$$

$$V_{Ui}\frac{dD_{Ui}}{dt} = \beta QD_{Li} - \beta QD_{Ui} + E_i V_{Ui}. \quad (6)$$

Under steady-state conditions, Equations 3–6 are equal to zero for each zone and yield a set of equations that can be solved through a Gaussian elimination technique, as shown in Noakes and Sleigh (2009) to find the dose or quanta concentration for each zone.

Infection risk model

Infection risk is modeled using the Wells–Riley equation (Riley et al. 1978). This relates the number of infective people in a space I, the room ventilation rate Q (m^3/s), and the quantity of infectious material in the air to predict the probability of infection (Pr) for a susceptible person over a period of time t (s):

$$\Pr = 1 - e^{-\frac{Iqpt}{Q}}. \quad (7)$$

Here p (m^3/s) is the pulmonary ventilation rate of susceptible individuals, while q represents the infectious quanta generation rate (quanta/s). Equation 7 can be related to Equation 3 by replacing the term qI/Q with the quanta concentration for each occupied lower zone C_{Li}. In each zone, the mean number of likely new cases of infection N_i over a time period t can be modeled by multiplying by the number of susceptible people in the zone S_i:

$$N_i = S_i\left(1 - e^{-C_{Li}pt}\right). \quad (8)$$

In all cases, a pulmonary ventilation rate of 10 L/min (0.35 cfm) is assumed, which is realistic for an adult. Infection risk is evaluated over a 24-h period, assuming continuous occupancy and quanta generation.

Energy

In each scenario, the energy requirements of the ventilation system and UVGI devices are assessed alongside the microbial removal performance. In all cases, it is assumed that ventilation is provided by mechanical means and that both the ventilation and UV systems operate continuously. Ventilation energy calculations follow Noakes et al. (2012); fan energy is assumed to require 2 W/l/s (56.6 W/ft^3/s), while ventilation heat loss is determined using the degree-day approach assuming 50% heat recovery and 2100 degree-days per year (typical for London, UK).

Energy consumption of the UV devices depends on the specific device power consumption, how much is converted to UV-C energy, and how well that is distributed within a room.

Table 1. Variation in energy performance and plane average irradiance with device and zone area.

Device	Power (W)	Coverage area, m^2 (ft^2)	E_{plane} (W/m^2)	Performance coefficient, η
WM136	36	4(43.1)	0.271	0.030
WM136	36	6.25(67.3)	0.173	0.030
WM136	36	9(96.9)	0.124	0.031
WM136	36	14(150.7)	0.09	0.035
WM236	72	4(43.1)	0.687	0.038
WM236	72	6.25(67.3)	0.472	0.041
WM236	72	9(96.9)	0.338	0.042
WM236	72	14(150.7)	0.267	0.052

Suitable values are determined for the current model by considering measured data from commercially available devices. As shown in Gilkeson and Noakes (2013), a UV device creates a 3D irradiance field in a room, typically concentrated over a narrow horizontal band with high irradiance close to the device and rapid decay governed by the inverse square law at increasing distance. The average field irradiance therefore depends on the number of devices and their particular location in a room. Values used here are based on the performance of two commercially available wall-mounted devices, Lumalier WM136 and WM236. Irradiance fields for these devices have been previously measured in a 3.35 m^3 (W) × 4.26 m^3 (L) × 2.26 m^3 (H) 11 ft^3 (W) × 14 ft^3 (L) × 7.4 ft^3 (H)) chamber and implemented as empirical models within a CFD model (Gilkeson and Noakes 2013). This model is used here to determine plane average irradiances E_{plane} (W/m^2) through the center of the devices mounted in differently sized zones. In each case, an energy performance coefficient η is calculated from the plane average irradiance, the area of the zone A (m^2), and the manufacturer supplied power consumption W (W) as

$$\eta = {}^{E_{plane}A}/_{W}. \tag{9}$$

Table 1 shows the plane average irradiance and performance coefficient for the two devices in four differently sized zones. It is clear that the performance depends on both the device and its location. The WM236 device contains twice the lamps and consumes twice the power of the WM136, but it is clearly more effective, as the average irradiance is between 2.5 and 2.9 times the irradiance in the same sized zone. It can also be seen that the relative energy performance varies within and between devices. Although the relationship between upper-zone irradiance and lamp power consumption is clearly not straightforward, it is necessary to assume a value for the purposes of carrying out energy calculations. In this case, a conservative value of $\eta = 0.03$ is chosen, based on the worst case in Table 1. This value is used in Equation 9 to calculate a suitable UV device power consumption for a given irradiance and room area specified in the model.

Multi-room application

The model is applied to a hypothetical six-zone hospital ward, as shown in Figure 2. It is assumed that there were six occupants in each of the four ward bays and two occupants (nursing staff) in each of the two corridor zones. Although continuous occupancy of a corridor zone may not be experienced in reality, it represents a worst-case scenario and is a reasonable approximation in the case where nursing stations or reception areas are located in these zones. Simulations assume there is one infectious person on the ward, located in ward bay 1 or in corridor zone 5. Ward bays have a floor area of 60 m^2 (646 ft^2) and corridor zones an area of 30 m^2 (323 ft^2). All zones are assumed to have a ceiling height of 2.7 m (8.86 ft), with the upper zone defined as the top 0.7 m (2.3 ft). Volume average irradiance E for this zone is calculated from a specified plane average E_{plane}, assuming that the UV device output is over a 10-cm (3.9-in.) band and that the average irradiance over this band was 60% of the peak value at the center. This is based on measurements (Gilkeson and Noakes 2013) that showed the peak was typically 57%–58% higher than the mean for the two devices tested in their study.

Infection risk calcuations are based on suitable parameters for tuberculosis (TB). Quanta generation rate for TB has been calculated in a number of studies and shown to vary substantially from 0.3–44 quanta per hour, with values over 200 quanta/h in the case of "superspreaders" (Escombe et al. 2009). In this study, a value of 12 quanta/h is used for the majority of models, based on calculations from an office outbreak reported by Nardell et al. (1991). A value of 50 quanta/h is applied in some scenarios to examine the influence of having a high generator. Susceptibility of *M. tuberculosis* bacteria

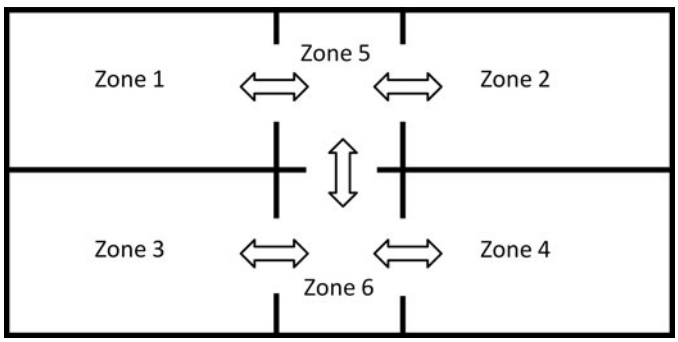

Fig. 2. Hypothetical ward layout showing inter-zone connections. Zones 1–4 are ward bays each containing six occupants; zones 5 and 6 are corridor/communal zones each containing two occupants.

Table 2. Ventilation, infector location, and UV scenarios for results in Figures 3 and 4.

Scenario	Ventilation rate (ACH)	Infector zone	UV	Inter-zone mixing, γ (m^3/s)
1a	3	1	None	0.1
1b				0.2
1c				0.01
2a	6	1	None	0.1
2b				0.2
2c				0.01
3a	3	1	Zone 1	0.1
3b				0.2
3c				0.01
4a	3	1	Zones 1–4	0.1
4b				0.2
4c				0.01
5a	3	1	Zones 5 and 6	0.1
5b				0.2
5c				0.01
6a	3	1	All zones	0.1
6b				0.2
6c				0.01
7a	3	5	None	0.1
7b				0.2
7c				0.01
8a	6	5	None	0.1
8b				0.2
8c				0.01
9a	3	5	Zone 1	0.1
9b				0.2
9c				0.01
10a	3	5	Zones 1–4	0.1
10b				0.2
10c				0.01
11a	3	5	Zones 5 and 6	0.1
11b				0.2
11c				0.01
12a	3	5	All zones	0.1
12b				0.2
12c				0.01

to UV-C irradiation also varies, with k-values in the range of 0.23–0.55 m^2/J as cited by National Institute for Occupational Safety and Health (NIOSH; 2009). Here a representative value for TB of 0.4 m^2/J is assumed for all calculations. Ventilation rates in the ward are assumed to be the same in all areas and varied between 3 and 15 AC/h. The mixing coefficient within each zone β is set at 3.5, based on typical values from CFD models for mechanically ventilated rooms in the absence of a mixing fan (Noakes et al. 2004b). Simulations are conducted for three values of the inter-zonal flow rate between the six zones of 0.01, 0.1, and 0.2 m^3/s (21.2, 212, and 424 cfm). These values were selected to represent three cases. The lowest value is equivalent to ~7.5% of the base ventilation rate of 3 AC/h in the ward areas and is intended to approximate a case where rooms are separated by closed doors but have no specific pressurization and doors are likely to be opened frequently and at times are left open for short periods. Eames et al. (2009) indicated that the exchanged volume from a door opening is up to 5% of the room volume; an exchange rate of 0.01 m^3/s is equivalent to seven to eight door movements in an hour assuming 3% of the room volume is moved. The two higher values of 0.1 and 0.2 m^3/s are intended to represent hospital wards with substantial mixing between the zones, which may occur where doors are permanently open or ward layouts that are separated into open bays with relatively free air paths between zones.

The model is initially run for the ventilation and air disinfection system scenarios set out in Table 2 for a single infector in either zone 1 or zone 5. Table 3 presents the calculated volume average UV dose for the six zones in each of the scenarios with UV devices present in Table 2. In each case, with UV devices active, an average plane irradiance through the center of the UV zone of 0.2 W/m^2 is assumed, based on a fairly conservative estimates from the range of values given in Table 1. For the cases with UV in all zones (scenarios 6–12), the dose is evenly distributed and is unaffected by the inter-zonal airflow. However, in other cases, the airflow has an influence on the dose distribution. This is particularly noticeable for scenarios 3 and 9, with UV only present in zone 1. At the two higher inter-zone flow rates, this device has a noticeable impact on neighboring spaces; however, at the lowest inter-zone flow rate, there is minimal influence of this UV device in the neighboring zones.

Results

Airborne pathogen distribution

Figure 3 shows the predicted distribution of airborne quanta for all the scenarios outlined in Table 2 for an infector in ward zone 1 (Figures 3a–3c) and an infector in corridor zone 5 (Figures 3d–3f). Quanta generation rate is 12 quanta/h, and quanta concentrations are normalized relative to the concentration in the infector zone in scenario 1a, with an inter-zone flow rate of 0.1 m^3/s (212 cfm). As expected, concentrations are highest close to the infectious patient (zones 1 or 5) and decrease with distance. Increasing the mixing between the zones reduces the concentrations in the source zone but increases concentrations in all other zones. Quanta concentrations are generally higher with an infector in the corridor zone than in a ward bay.

It can be seen in both infector scenarios that all interventions are beneficial compared to scenario 1a (3 air changes per hour [ACH], with no UV), with the most effective approaches doubling the air change rate (scenarios 2 and 7) or adding UV devices into all zones (scenarios 6 and 12). In the case where the infector is located in ward zone 1, adding UV devices to this zone and to all ward zones is also effective. Adding UV devices in the corridor zones is less effective, although it still has a clear benefit for all but the source zone. In the case of an infector in the corridor zone, the addition of UV in the corridor is more beneficial than when an infector is in a ward, but the greatest quanta reductions are predicted with UV devices added to all wards or all zones. The results also indicate that in the case with the lowest inter-zonal flow rate, interventions are only effective where they are applied in the infector zone,

Table 3. Calculated UV dose distributions for results in Figures 3 and 4.

	Volume average UV dose (J/m^2)					
Scenario	Zone 1	Zone 2	Zone 3	Zone 4	Zone 5	Zone 6
3a/9a	2.292	0.148	0.039	0.039	0.549	0.144
3b/9b	1.993	0.264	0.093	0.093	0.620	0.220
3c/9c	2.770	0.006	0.0003	0.0003	0.157	0.009
4a/10a	2.518	2.518	2.518	2.518	1.385	1.385
4b/10b	2.444	2.444	2.444	2.444	1.680	1.680
4c/10c	2.781	2.781	2.781	2.781	0.333	0.333
5a/11a	0.346	0.346	0.346	0.346	1.479	1.479
5b/11b	0.420	0.420	0.420	0.420	1.184	1.184
5c/11c	0.083	0.083	0.083	0.083	2.531	2.531
6a/12a	2.864	2.864	2.864	2.864	2.864	2.864
6b/12b	2.864	2.864	2.864	2.864	2.864	2.864
6c/12c	2.864	2.864	2.864	2.864	2.864	2.864

and there is only a minimal benefit on neighboring zones. This is not surprising, as limiting the airflow between zones is providing the bulk of the protection to occupants located away from the infectious source.

Energy and infection risk

Although the results in Figure 3 give an insight into the distribution of an airborne pathogen in the different scenarios, selecting a suitable intervention requires considering what this means in terms of infection risk and the resource implications of each of the schemes. Figure 4 shows the predicted annual energy consumption and total number of new infection cases in a 24-h period for scenarios 1a–6c in Table 2, with an infector in ward zone 1 generating 12 quanta/h. It can be seen that in all cases, the lowest infection risk occurs with a ventilation rate of 3 ACH and UV devices operating in all rooms (scenario 6), yet the energy use in this case is high. The lowest energy on the other hand is scenario 1 with a low air change rate and no UV devices, but this has the highest infection risk in all cases. All scenarios with UV devices active result in an energy consumption that is less than increasing the air change rate to 6 ACH, and in the case of scenarios 4 and 6, the infection risk is also lower. This gives support to the potential for UVGI be a more energy-efficient form of infection control than the conventional approach of increasing the fresh air exchange rate. The results also give further insight into the benefits in different designs of environments. It can be seen in all cases that an increased inter-zonal airflow rate results in an increase in likely infection risk for the same energy, despite Figure 3 showing that the risk close to the source patient is likely to decrease. However the additional benefit derived from multiple UV fixtures, when the infector zone is known, is only apparent where there is high air exchange between zones. With a low inter-zone air exchange rate, installing UV in the infector zone (scenario 3c) is likely to reduce infection risk significantly for only a small increase in energy consumption compared to ventilation alone. However in this case, application of UV devices in other zones (4c AND 6c) has only a small predicted benefit from an infection control perspective.

Figure 5 considers the influence of disease and infector parameters. In Figure 5a, results are presented to compare infection risk and energy for the scenarios in Table 2 at an inter-zonal flow rate of 0.1 m^3/s with the infector in zone 1 (scenarios 1a–6a) or zone 5 (7a–12a). It can be seen that at 3 ACH with no UV (scenarios 1a and 7a), the overall risk is similar regardless of the location of the infector. In scenarios 2a, 8a, 6a, and 12a, the risk is lower with the infector in zone 5 rather than zone 1, while in scenarios 4a and 10a, the risk is lower when the infector is in zone 1. In the case of scenarios 3a, 9a, 5a, and 11a, both have comparable energy requirements yet, there is a substantial difference in infection risk depending on the location of the infector. This is logical, as in all scenarios the infection risk is lowered when a UV device is placed in the infector zone. Figure 5b gives some insight into the disease parameters by running scenarios 1a–6a considering a normal (12 quanta/h) and high (50 quanta/h) quanta generation rates. The results indicate that the relative impact of all the interventions is the same; however, the effectiveness in practice will depend on the disease characteristics.

The results in Figures 4 and 5 indicate that installation of a UV system may be a more energy-efficient option for infection control than increasing ventilation. The results, however, indicate that there is always a trade-off between the investment of energy requirements and the infection risk, and the most suitable system is not immediately apparent. The most appropriate system will depend on the disease, ward design, and occupants and may be a combination of increased ventilation with UV in one or more zones.

To explore this further a parametric study was carried out to investigate the relative contribution of UV and ventilation combined to both energy and infection risk. An extended optimal Latin hypercube (EOLH) technique (Toropov et al. 2007) was used to create a design of experiments to sample potential design options with an air change rate between 3 and 12 ACH and UV with an average plane irradiance of 0.2 W/m^2 in any single zone, in the two corridor zones (5 and 6), or in all the ward zones (1–4). The model assumed an inter-zonal flow rate of 0.1 m^3/s and an infector in zone 1 with a quanta generation rate of 12 quanta/h. For each combination of parameters,

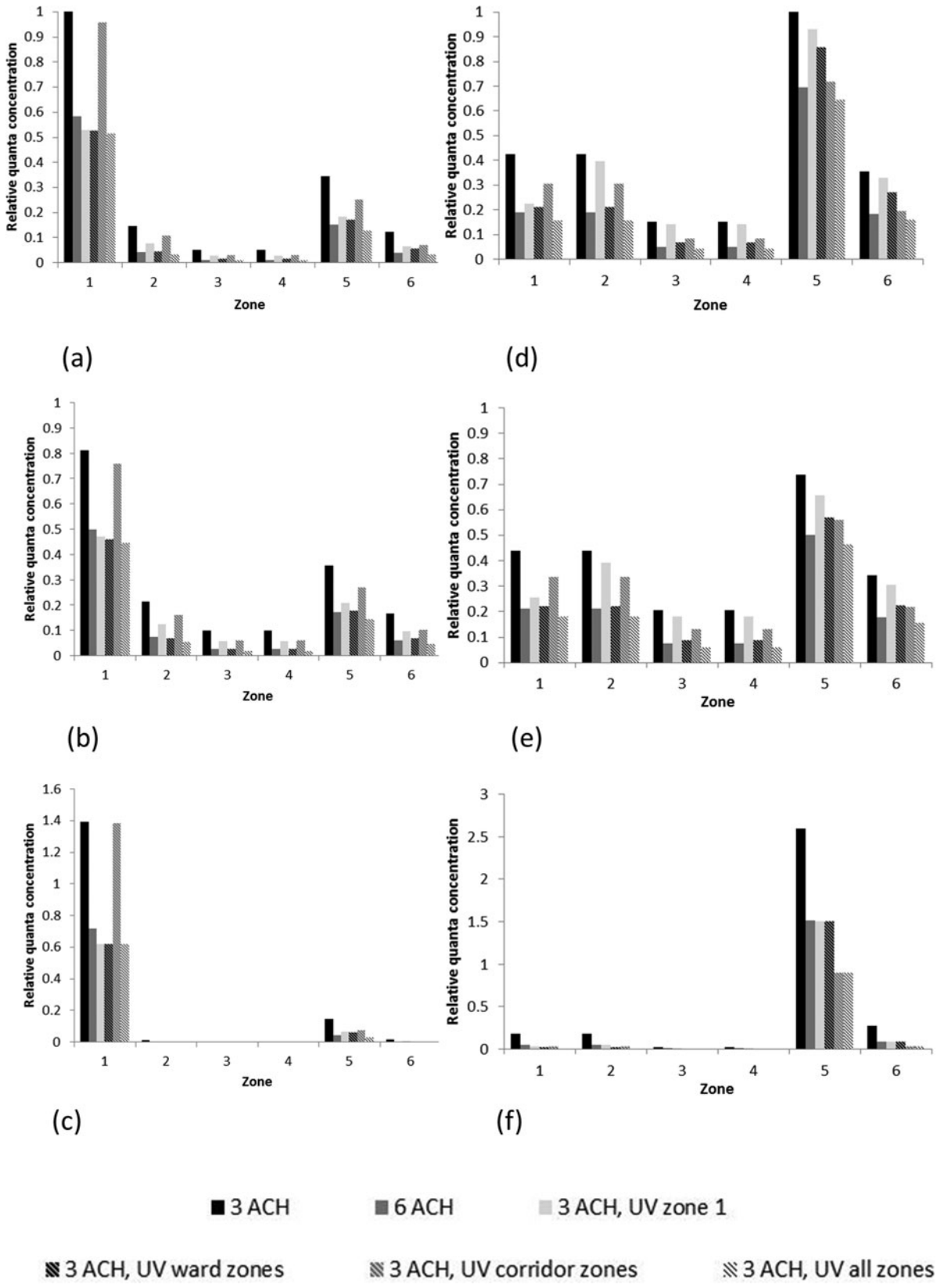

Fig. 3. Impact of ventilation rate, inter-zonal mixing, UV device operation, and infector location on relative airborne quanta concentration in all six zones. a. Inter-zone flow rate 0.1 m^3/s, infector zone 1. b. Inter-zone flow rate 0.2 m^3/s, infector zone 1. c. Inter-zone flow rate 0.01 m^3/s, infector zone 1. d. Inter-zone flow rate 0.1 m^3/s, infector zone 5. e. Inter-zone flow rate 0.2 m^3/s, infector zone 5. f. Inter-zone flow rate 0.01 m^3/s infector, zone 5.

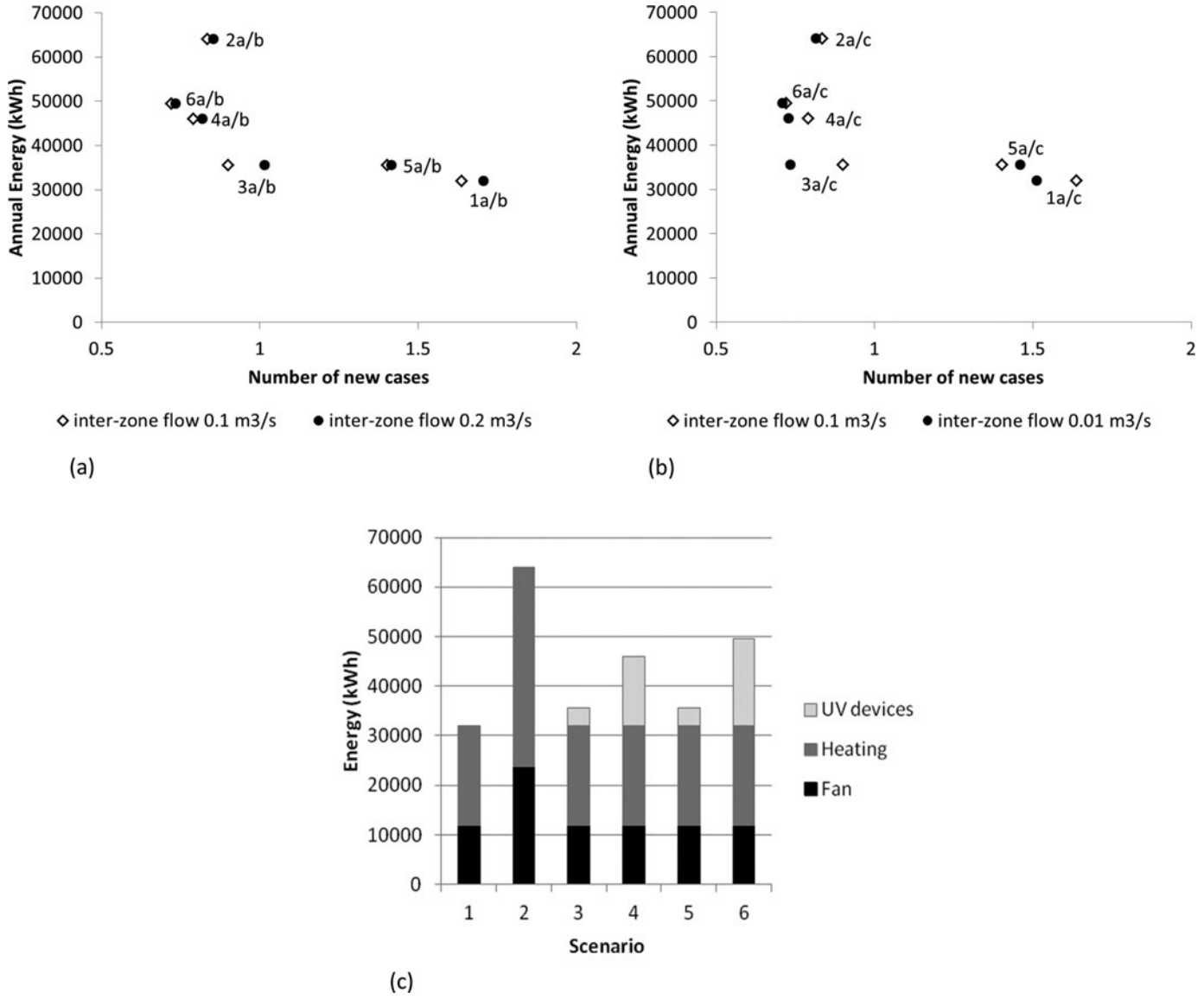

Fig. 4. Infection risk and energy use for scenarios 1a–6c. a. Infection risk over a 24-h period compared to annual energy for interzonal flow rates of 0.1 and 0.2 m^3/s. b. Infection risk over a 24-h period compared to annual energy for interzonal flow rates of 0.1 and 0.01 m^3/s. c. Annual energy consumption for the six scenarios.

the 24-h infection risk and annual energy was calculated and plotted in terms of the percent of increase in energy and percent of reduction in infection based on the case with 3 ACH and no UV devices. The change and infection risk resulting from an increase in ventilation rate only is also plotted. The simulated design options are shown in Figure 6.

It can be seen from the results in Figure 7 that the relationship between energy and predicted number of cases follows two clusters of curves. The solid line results from increasing air change rate alone, and the other points clustered near this line result from adding devices in zones where there is no infector. It can be seen that just adding a device in a single zone where there is no infector (zones 2 and 4 shown) has no benefit for a given energy consumption and, in some cases, requires more energy than would be needed to achieve the same infection reduction using ventilation alone. Installing devices in the corridor (zones 5 and 6) has a marginal benefit in terms of reducing infection at the same energy cost with a greater effect at lower air change rates. The second curve is generated where there is a UV device in the source zone (zone 1), with the points separated to show this zone only and addition of devices in all patient zones. Energy consumption is dominated by ventilation, with the UV devices contributing between 3500 and 14,000 kWh (11.9 to 47.8 MBtu) to the total consumption.

Discussion

The study presented here shows that it is feasible to extend zonal models for upper-room UV device performance that have previously been applied to single zones to a multizone environment, such as a hospital ward. The study also

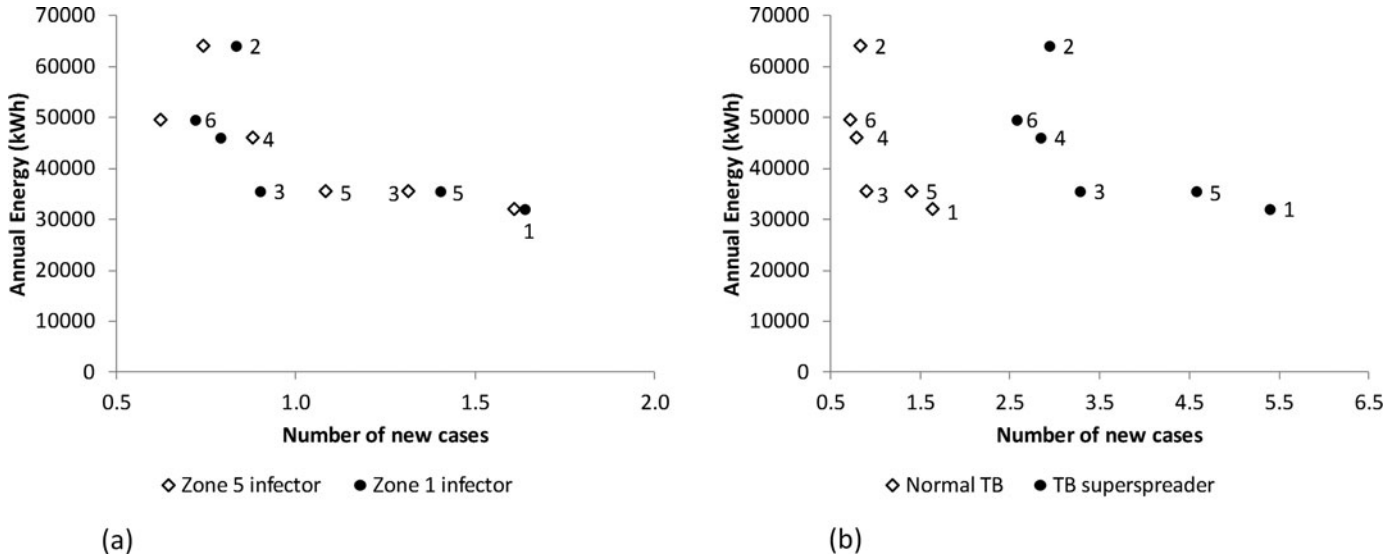

Fig. 5. Infection risk compared to energy for the scenarios in Table 2 at an inter-zonal flow rate of 0.1 m^3/s. a. Influence of infector location. b. Influence of quanta generation rate.

shows that by considering energy and infection risk together, it is also possible to compare different design approaches at a whole environment level in terms of their infection control benefits and additional energy requirements. Although the model framework presented here offers a potential approach to assessing feasibility of an infection control system, it is important to consider the validity of the models and the limitations in the physics and applicability of the model.

UV disinfection model

The model presented here applies a first-order decay model to simulate the inactivation of microorganisms in response to a UV field. This model is widely applied in assessing in-duct (Kowalski 2009) and upper-room (Noakes et al. 2004a; Miller et al. 2002; Nicas and Miller 1999) UV disinfection devices and can be applied with a reasonable degree of confidence to a range of microorganisms. The model is based on numerous experimental observations of the UV disinfection process in laboratory environments (Riley et al. 1976; Ko 2000; Peccia and Hernandez 2001, 2002; Xu et al. 2003) with microorganism susceptibility data also derived from experimental studies. Although studies report some variation in susceptibility values (Kowalski 2009), for most microorganisms, the reported data are similar between studies. In the case of TB considered here, Riley et al. (1976) reported a susceptibility constant of 0.47 m^2/J, which is consistent with the range of 0.23–0.55 m^2/J indicated by NIOSH (2009). As *Mycobacterium tuberculosis* is a difficult and dangerous microorganism

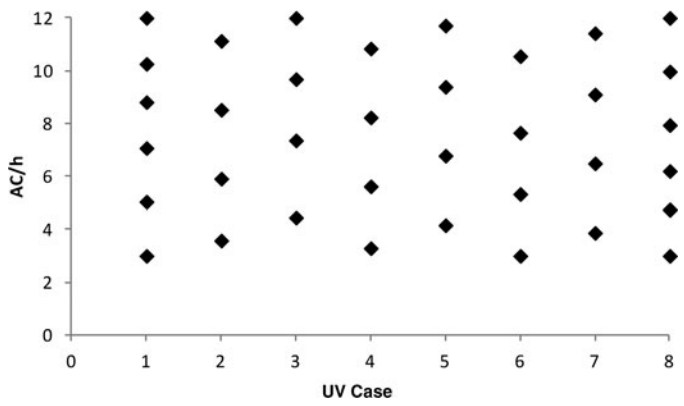

Fig. 6. EOLH (Toropov et al. 2007) design of experiments based sampling of potential design options for ACH and UV in different zones. Here UV cases 1–6 represent UV in single zones 1–6, case 7 represents UV in the two corridor zones (5 and 6), and case 8 represents UV all ward zones (1–4).

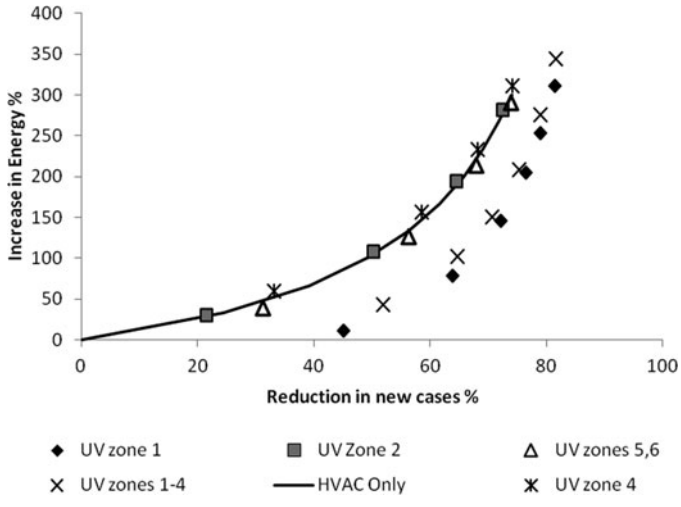

Fig. 7. Infection risk compared to energy for ventilation 3–15 ACH and UV in one or more zones.

to work with, many researchers have based analysis on related species, with k-values in the range 0.12–0.24 m^2/J reported for *Mycobacterium bovis* BCG (Riley et al. 1976; Ko 2000; Peccia and Hernandez 2002) and 0.12–0.18 m^2/J reported for *Mycobacterium parafortuitum* (Peccia and Hernandez 2001; Xu et al. 2003). Although the k-values are slightly lower, these two surrogate species show consistent behavior, are of an order of magnitude similar to TB, and are widely used in laboratory UV assessments. Susceptibility data are available for a number of other bacteria and fungi in air, including *Serratia marcesens*, *Escherichia coli*, *Pseudomonas aeruginosa*, *Staphyloccus aureus*, and *Aspergillus* spp (Kowalski 2009). Data are also available for some viruses; however, there are only limited data on the susceptibility of some important respiratory pathogens, including influenza (Jensen 1964).

Zonal modeling approach

The zonal modeling approach has two aspects that need to be considered: the means of modeling the movement of air and airborne microorganisms within a building and the validity of assuming a room can be treated as a two-zone space with a uniform upper-room UV field to model the disinfection process. In terms of modeling the building airflow, the approach applied here is considerably simplified. In a real environment, ventilation rates in different spaces are unlikely to be the same and may vary between neighboring rooms depending on design, occupancy, and weather. The flow within a zone will be affected by thermal plumes from people and equipment; in many cases, this will promote mixing and will be beneficial, but in some cases, for example, with displacement flows, it may be detrimental to infection control (Li et al. 2011). The flow between zones will depend not only on the layout and ventilation design but also on the movement of people between zones and whether doors are opened or closed. The model here assumes a steady-state environment that may be realistic for mechanically ventilated rooms with stable occupancy. However, in cases with high activity or natural ventilation, flows are likely to be dynamic and less predictable, although several studies have shown that high ventilation rates can be achieved in naturally ventilated environments (Qian et al. 2010; Gilkeson et al. 2013). The simplified airflow model is deliberately adopted here to demonstrate the behavior of the various parameters that determine upper-room UV performance in a simplified environment without dealing with the complications and computational requirements of modeling and evaluating transient airflow in real environments. Through parametric study, the relative influence of ventilation rate and inter-zone flow parameters are considered and shown to be significant factors in design. Application of the approach to a real environment would benefit from a more accurate modeling approach to evaluate the building specific airflow pathways and, hence, the likely distribution of any airborne contaminant. This could be done through a ventilation network model, such as CONTAM, or one of the many commercially available building simulation tools or even modeling a ward zone within a CFD simulation to assess the likely spatial distribution of infectious material in a real situation. In the case of CFD approaches, steady-state airflow models without the movement of people have been shown to have reasonable correlation with infection cases seen in ward (Wong et al. 2010) and building (Yu et al. 2004) outbreaks.

Applying a two-zone model within each room space to simulate the UV disinfection process has been shown in a previous study to give realistic predictions. Although the model does not capture the detail of the airflow patterns, comparison with CFD simulations that include both the 3D airflow patterns and 3D UV fields (Noakes et al 2004b) shows that with an appropriate mixing coefficient β, the zonal model is capable of accurately predicting the zone average concentrations in the upper and lower zones of the room. The value of $\beta = 3.5$ selected in the current study is based on values derived from CFD models (Noakes et al. 2004b) and is representative of a room with a dilution ventilation system that has reasonable, but incomplete, mixing. Higher levels of mixing, represented by higher values of β, increase the effectiveness of the upper-room UV devices; the value selected here is a realistic but fairly conservative choice. CFD or experimental studies of room airflows with different ventilation systems and/or heat loads would enable determination of values of β for different cases.

In the current study, all simulations were conducted with a plane average UV irradiance of 0.2 W/m^2 in scenarios with UV present. This was selected based on likely performance of commercially available devices derived from measurements (Gilkeson and Noakes 2013). Although the influence of this parameter was not considered in the current study, the value selected is realistic and is below the plane average irradiance of 0.3–0.5 W/m^2 recommended by NIOSH (2009), and it therefore represents a reasonably conservative estimate of the UV irradiance that can be achieved. The actual plane irradiance in a particular room will depend on both the choice of upper-room UV device and the placement relative to the geometry of the room. CAD models incorporating ray-tracing can be used to determine UV field distributions for different fixtures and room layouts (Rudnick et al. 2012). However, the disinfection capability also depends on the interaction of the UV field with the airflow; CFD simulations show that the same device placed in a different location relative to the ventilation flow can result in substantially different UV doses (Noakes et al. 2006).

Infection model

The Wells–Riley model applied to estimate infection risk has been widely applied, particularly in TB studies, but has also been recognized as having limitations. The model is uncertain for transient and small populations where stochastic effects are important in the transmission process (Noakes and Sleigh 2009). The model is based on Wells's (1955) concept of defining a "quanta" of infection, which is an approximation of the real infection process, combining the pathogen virulence and concentration as well as the host response. Quanta values are typically calculated from past outbreaks, which may be based on unreliable outbreak or ventilation data. While there are several studies that report quanta values for TB (Nardell

et al. 1991; Beggs et al. 2003; Escombe et al. 2007, 2008), there are limited data for other pathogens. Values have been reported for influenza (Rudnick and Milton 2003; Liao et al. 2005), measles (Riley et al. 1978), and SARs (Liao et al. 2005), which could, with appropriate UV susceptibility data, be used to conduct preliminary assessments into effectiveness against these pathogens. However, further data would be required to carry out reliable calculations relating to infection risk for other diseases. The model also has limitations in application to pathogens where infection cannot be assumed to be represented as an exponential dose-response, where a single large dose of infectious material is the same as smaller doses arriving over a shorter time period (Pujol et al. 2009). These issues were discussed in some detail in Noakes and Sleigh (2009). Development of a stochastic version of the present model would be a beneficial future development to deal with small populations and better characterize uncertainty in the results (Noakes and Sleigh, 2009; Noakes et al. 2012). Application of dose-response type approaches (Pujol et al. 2009; Armstrong and Haas 2007; Jones et al. 2009) may also offer a future option for model development.

Energy assumptions

The energy calculations carried out here are based on an assumed consumption for ventilation flows, the widely applied degree-day method for heat loss and manufacturer data for the UV devices. While the relative magnitudes of these parameters are realistic, the actual energy consumption will be case specific, depending on the particular system design, local climate, and operation and maintenance. In the case of the UV devices, the results presented in this study are based on two commercially available devices. While this means there is reasonable confidence in the energy calculations for these particular fixtures, the values may not be representative of all UV devices. There are many designs of devices on the market suited to different shapes of rooms and ceiling heights, including some that have greater energy efficiency than those applied in this study. In applying the model to a real environment, a more detailed energy assessment using a comprehensive building energy simulation tool and/or measured consumption data would be essential.

Model application

The results presented demonstrate the potential of the modeling approach to inform design decisions. Despite the limitations outlined above and the uncertainties in some of the parameters, the model presents an approach to explore the relationship between different design parameters. By considering steady-state conditions with continuous occupancy and, in many cases, conservative parameter estimates, the results represent a worst-case scenario. In addition, while the specific infection risks may vary, the relative benefits of different system options are consistent.

An ideal design is likely to be one that minimizes both energy and the transmission of infection. However as the results show, there is no universal optimum point; hence, the best design will depend on the particular set of requirements and the most appropriate trade-off. As can be seen from Figures 4 and 5, installation of a UV device in the source zone (scenarios 3 or 5 depending on infector location) results in arguably the most reasonable trade-off, with both relatively low infection risk and energy requirement. However, this is not necessarily a robust solution; it relies on knowing a patient is infectious and being able to locate them accordingly. This same behavior is apparent in Figure 6; the zone 1 points on the lower curve, while closer to an optimum solution, rely on knowledge of a patient being infectious. It can be seen that installing UV devices in all patient rooms potentially offers a more robust solution, particularly if the location of an infector is not known; this corresponds to scenario 4 in Figures 4 and 5. This appears to be more effective for a given energy cost than installing UV devices in communal areas, and the two cases here suggest that this is regardless of the location of the infector.

As shown in Figure 5b, the infection is also likely to play a role in the decision process. All simulations conducted here model the infection risk for a normal TB patient in terms of new cases over a 24-h period yet calculate the energy requirement over a year. This approach is taken based on the assumption that for most hospital wards, the presence of an actively infectious TB patient is rare but may happen. Investment in systems is therefore justified to prevent the costs of treating even a small number of cases, and at the same time, reduces broader risks associated with other pathogens. However, in some environments, the likelihood of an infector being present or the chance of particularly virulent and difficult to treat strains being present may be that much higher that investment in substantially higher ventilation rates and/or higher powered air disinfection systems may be warranted.

Current approaches to designing healthcare environments for infection control are based on national guidance, such as that provided by ASHRAE and ASHE in the United States (ASHRAE 2013) and the Department of Health in the United Kingdom (Department of Health 2007). Design is typically based on recommendations for minimum ventilation rates in different clinical environments and calculation of risk, and the relationship to design and energy consumption is not routinely carried out. In the case of a high risk of airborne infection, negative pressure isolation facilities at high ventilation rates are recommended; however, this assumes rapid identification and isolation of all infectious patients. Making a decision on suitable ventilation and whether or not to install additional protection, such as upper-room UV, is not straightforward and will depend on many factors, including the ability to treat an infection, likelihood of passing on to others, patient cohort, design of the environment, pressure an infection case places on a health service, and capability of an organization to install and maintain different types of infection control systems. Cost will inevitably be a factor, and it may seem that conducting a cost–benefit analysis to examine the trade-off between infection control and equipment, maintenance, and energy needs would enable identification of optimum design. However this is far from straightforward. Costing the purchase, installation, and operation of a ventilation or UV disinfection system is case and country specific, but it is feasible using

current industry approaches. However, as shown in Noakes et al. (2012), putting a cost to treating infection is very subjective, depending on the specific infection, hospital operation and management, and the wider societal and economic impacts of infection cases.

Future development

As highlighted above, the model developed here is applied to a theoretical airflow environment to explore the model behavior. A number of the model elements have been widely applied in other research studies, and several, including the UV disinfection models, have been validated against experimental and/or CFD simulation studies. A more detailed validation of UV zonal models in a standalone experimental room can be achieved (Beggs et al. 2006). There is a need for a full validation of this model in a real ward setting; however, this is a considerable challenge and may even be impossible. As the model stands, it enables exploration of the parameters that are important in selecting an appropriate infection control system and considers infection control and energy requirements of a system together. Future development of the model to include stochastic effects, characterize uncertainty, and incorporate a more realistic building airflow model would allow the approach to be used in the future to conduct design assessments.

Conclusion

The model presented in this study provides a framework for evaluating the potential benefits of upper-room UV devices by combining zonal models of building airflow, UV disinfection models, the Wells–Riley model of infection risk, and calculation of energy use to consider infection risk and energy requirements of different scenarios at the same time. Although the model has its limitations, it provides valuable insight into the inter-play between ward design, ventilation, disease, and device parameters. The results suggest that installation of upper-room UV may be a more energy-efficient solution of achieving the same or better reduction in airborne infection risk than increasing ventilation rates. Installation in a source patient zone generally yields the greatest benefit for the smallest outlay; however, where the location of infectious patients is not known, installation of upper-room UV devices in patient areas is a more robust solution. While minimizing inter-zonal transfer between areas reduces infection risk, the results indicate that UV disinfection may be particularly beneficial in hospital areas with semi-open design where there is likely to be substantial air transfer between spaces. This may be relevant in minimizing opportunist infections in multi-occupant ward environments where patients are co-located in open bays or in waiting areas or emergency rooms where simple partitions or curtains are used to separate spaces.

The ideal solution will clearly depend on the particular environment, the particular infection, and considerations around capital costs, maintenance costs, and in some cases, the ease of retrofitting. However, the model illustrates the feasibility of applying air-cleaning technologies as an energy-efficient solution to controlling infection and shows that considering the whole ward rather than just a single room may allow a more robust system to be installed. This is the case for both ventilation and air-cleaning approaches and demonstrates the need to consider how rooms within a healthcare environment inter-play to tackle both energy use and infection control.

Acknowledgments

Further information on the models and the data in the paper can be obtained by contacting the authors.

Funding

The authors would like to acknowledge the support of the UK Engineering and Physical Sciences Research Council (EPSRC) for funding this study.

References

Armstrong, T.W., and C.N. Haas. 2007. A quantitative microbial risk assessment model for Legionnaires' disease: Animal model selection and dose-response modelling. *Risk Analysis* 27:1581–96.

ASHRAE. 2013. *ANSI/ASHRAE/ASHE Standard 170-2013, Ventilation of Health Care Facilities*. Atlanta: ASHRAE.

Beggs, C.B., C.J. Noakes, P.A. Sleigh, L.A. Fletcher, and K.G. Kerr. 2006. Methodology for determining the susceptibility of airborne microorganisms to irradiation by an upper-room UVGI system. *Journal of Aerosol Science* 37(7):885–902.

Beggs, C.B., and P.A. Sleigh. 2002. A quantitative method for evaluating the germicidal effect of upper room UV fields. *Journal of Aerosol Science* 33:1681–99.

Beggs, C.B., C.J. Noakes, P.A. Sleigh, L.A. Fletcher, and K. Siddiqi. 2003. The transmission of tuberculosis in confined spaces: an analytical study of alternative epidemiological models. *International Journal or Tuberculosis and Lung Disease* 7:1015–26.

Department of Health. 2007. Specialised ventilation for healthcare premises, Part A: Design and validation, Health Technical Memorandum HTM 03-01, The Stationary Office, London.

Eames, I., J.W. Tang, Y. Li, and P. Wilson. 2009. Airborne transmission of disease in hospitals. *Journal of the Royal Society Interface* 6(Suppl 6):S697–702.

Escombe, A.R., D.A.J. Moore, R.H. Gilman, M. Navincopa, E. Ticona, B. Mitchell, C.J. Noakes, C. Martínez, P. Sheen, R. Ramirez, W. Quino, A. Gonzalez, J.S. Friedland, and C.A. Evans. 2009. Upper-room ultraviolet light and negative air ionization for the prevention of airborne tuberculosis transmission. *PLOS Medicine* 6(3):e1000043.

Escombe, A.R., D.A.J. Moore, R.H. Gilman, W. Pan, M. Navincopa, E. Ticona, C.Martinez, L. Caviedes, P. Sheen, A. Gonzalez, C.J. Noakes, J.S. Friedland, and C.A. Evans. 2008. The infectiousness of tuberculosis patients coinfected with HIV. *PLOS Medicine* 5:1387–97.

Escombe, A.R., C. Oeser, R.H. Gilman, M. Navincopa, E. Ticona, C. Martinez, L. Caviedes, P. Sheen, A. Gonzalez, C.J. Noakes, D.A.J. Moore, J.S. Friedland, and C.A. Evans. 2007. The detection of airborne transmission of tuberculosis from HIV-infected patients, using an in vivo air sampling model. *Clinical Infectious Diseases* 44:1349–57.

Gilkeson, C.A., M.A. Camargo-Valero, L.E. Pickin, and C.J. Noakes. 2013. Measurement of ventilation and airborne infection risk in large naturally ventilated hospital wards. *Building and Environment* 65:35–48.

Gilkeson, C.A., and C.J. Noakes. 2013. Application of CFD simulation to predicting upper-room UVGI effectiveness. *Photochemistry and Photobiology* 89(4):799–810.

Jensen, M.M. 1964. Inactivation of airborne viruses by ultraviolet irradiation. *Applied Microbiology* 52:418–20.

Jones, R.M., Y. Masago, T.A. Bartrand, C.N. Haas, M. Nicas, and J.B. Rose. 2009. Characterizing the risk of infection from *Mycobacterium tuberculosis* in commercial passenger aircraft using quantitative microbial risk assessment. *Risk Analysis* 29: 355–65.

Ko, G., M.W. First, and H.A. Burge. 2000. Influence of relative humidity on particle size and UV sensitivity of *Serratia marcescens* and *Mycobacterium bovis* BCG aerosol. *Tubercle and Lung Disease* 80:217–28.

Kowalski, W. 2009. *Ultraviolet Germicidal Irradiation Handbook*. Springer-Verlag, Berlin Heidelberg.

Li, Y., P.V. Nielsen, and M. Sandberg. 2011. Displacement ventilation in hospital environments. *ASHRAE Journal* 53(6):86–8.

Liao, C.M., C.F. Chang, and H.M. Liang. 2005. A probabilistic transmission dynamic model to assess indoor airborne infection risks. *Risk Analysis* 2:1097–107.

Miller, S.L., M. Hernandez, K. Fennelly, J. Martyny, J. Macher, and E. Kujundzic. 2002. Efficacy of ultraviolet irradiation in controlling the spread of tuberculosis. NIOSH final report, Contract 200–97–2602, NTIS publication PB2003-103816, U.S. Department of Health and Human Services, Centers for Disease Control and Prevention, Cincinnati, OH.

Nardell, E.A., J. Keegan, S.A. Cheney, and S.C. Etkind. 1991. Airborne infection: Theoretical limits of protection achievable by building ventilation. *American Review of Respiratory Disease* 144:302–6.

National Institute for Occupational Safety and Health (NIOSH). 2009. Environmental control for tuberculosis: Basic upper-room ultraviolet germicidal irradiation guidelines for healthcare settings. Centers for Disease Control and Prevention, National Institute for Occupational Safety and Health, Washington DC.

Nicas, M., and S.L. Miller. 1999. A multi-zone model evaluation of the efficacy of upper-room air ultraviolet germicidal irradiation. *Applied and Occupational Environmental Hygiene* 14:317–28.

Noakes, C.J., C.B. Beggs, and P.A. Sleigh. 2004a. Effect of room mixing and ventilation strategy on the performance of upper room ultraviolet germicidal irradiation systems. *ASHRAE IAQ Conference, Tampa, FL, March 15–17*.

Noakes, C.J., C.B. Beggs, and P.A. Sleigh. 2004b. Modelling the performance of upper room ultraviolet germicidal irradiation devices in ventilated rooms: Comparison of analytical and CFD methods. *Indoor and Built Environment* 13:477–88.

Noakes, C.J., and P.A. Sleigh. 2009. Mathematical models for assessing the role of airflow on the risk of airborne infection in hospital wards. *Journal of the Royal Society Interface* 6:S791–800.

Noakes, C.J., P.A. Sleigh, L.A. Fletcher, and C.B. Beggs. 2006. Use of CFD modelling to optimise the design of upper-room UVGI disinfection systems for ventilated rooms. *Indoor and Built Environment* 15(4):347–56.

Noakes, C.J., P.A. Sleigh, and A. Khan. 2012. Appraising healthcare ventilation from combined infection control and energy perspectives. *HVAC&R Research* 18(4):658–70.

Peccia, J., and M. Hernandez. 2001. Photoreactivation in airborne *Mycobacterium parafortuitum*. *Applied and Environmental Microbiology* 67:4225–32.

Peccia, J., and M. Hernandez. 2002. UV-induced inactivation rates for airborne *Mycobacterium Bovis* BCG. *Journal of Occupational and Environmental Hygiene* 1(7):430–5.

Pujol, J.M., J.E. Eisenberg, C.N. Haas, and J.S. Koopman. 2009. The effect of ongoing exposure dynamics in dose response relationships. *PLoS Computational Biology* 5:e1000399.

Qian, H., Y. Li, W.H. Seto, P. Ching, W.H. Ching, and H.G. Sun. 2010. Natural ventilation for reducing airborne infection in hospitals. *Building and Environment* 45(3):559–65.

Riley, E.C., G. Murphy, and R.L. Riley. 1978. Airborne spread of measles in a suburban elementary school. *American Journal of Epidemiology* 107:421–32.

Riley, R.L., M. Knight, and G. Middlebrook. 1976. Ultraviolet susceptibility of BCG and virulent tubercle bacilli. *American Review of Respiratory Disease* 113:413–8.

Riley, R.L., and S. Permutt. 1971. Room air disinfection by ultraviolet irradiation of upper air. *Archives of Environmental Health* 22:208–19.

Rudnick, S.N., M.W. First, T. Sears, R.L. Vincent, P.W. Brickner, and P.Y. Ngai. 2012. Spatial distribution of fluence rate from upper-room ultraviolet germicidal irradiation: Experimental validation of a computer-aided design tool. *HVAC&R Research* 18(4):774–94.

Rudnick, S.N., and D.K. Milton. 2003. Risk of airborne infection transmission estimated from carbon dioxide concentration. *Indoor Air* 13:237–45.

Sung, M., and S. Kato. 2010. Method to evaluate UV dose of upper-room UVGI system using the concept of ventilation efficiency. *Building and Environment* 45:1626–31.

Toropov, V.V., S.J. Bates, and O.M. Querin. 2007. Generation of extended uniform Latin hypercube designs of experiments. *Proceedings of the Ninth International Conference on the Application of Artificial Intelligence to Civil, Structural and Environmental Engineering, Stirlingshire, Scotland, UK*.

Wells, W.F. 1955. *Airborne contagion and air hygiene*. Cambridge, MA: Harvard University Press.

Wong, B.C., N. Lee, Y. Li, P.K. Chan, H. Qiu, Z. Luo, R.W. Lai, D.S. Hui, K.W. Choi, and I.T. Yu. 2010. Possible role of aerosol transmission in a hospital outbreak of influenza. *Clinical Infectious Diseases* 51(10):1176–83.

Xu, P.J., J. Peccia, P. Fabian, J.W. Martyny, K.P. Fennelley, M. Hernandez, and S.L. Miller. 2003. Efficacy of ultraviolet germicidal irradiation of upper-room air in inactivating airborne bacterial spores and mycobacteria in full-scale studies. *Atmospheric Environment* 37:405–19.

Yu, I.T.S., Y.G. Li, T.W. Wong, W. Tam, A.T. Chan, J.H.W. Lee, D.Y.C. Leung, and T. Ho. 2004. Evidence of airborne transmission of the severe acute respiratory syndrome virus. *New England Journal of Medicine* 350(17):1731–9.

Zhu, S., J. Srebric, S.N. Rudnick, R.L. Vincent, and E.A. Nardell. 2013. Numerical investigation of upper-room UVGI disinfection efficacy in an environmental chamber with a ceiling fan. *Photochemistry and Photobiology* 89(4):782–91.